

Evaluation of the Physicochemical Parameters of a Variety of Okra: Clemson Spineless

Bienvenu Magloire Pakouzou^{1,2}, Vinci de Dieu B. Bokoyo^{1,2}, Thierry S. Gbembongo¹, Moctar Ousman^{2,3}, Venant S. Chara-Dackou¹, Timoléon M'Baïkoua¹ and Dieudonné J. Bathi ébo²

1. *Laboratoire d'Energétique Carnot, Faculté des Sciences, Université de Bangui, BP 1450 Bangui, Centrafrique*

2. *Laboratoire d'Energies Thermiques Renouvelables, Université J. Ki-Zerbo, 10 BP 13 495 Ouaga 10, Burkina Faso*

3. *University of Agadez, P.O. Box 199, BP 1000 Agadez, Niger*

Abstract: Significant quantities of okra rot during harvest periods due to a lack of appropriate technology for processing and preserving these products. To remedy this, this article proposes a CPC (cylindrical parabolic collector) solar dryer for drying a variety of okra (Clemson Spineless). This solar equipment consists of two parts: the drying chamber and the reflector concentrator unit. The coaxial tubular reflector is wrapped in small pieces of transparent glass that are opaque to infrared rays, limiting enormous radiative and convective losses. The greenhouse effect this creates helps to increase the air temperature, both in the receiver and inside the drying chamber, thus promoting natural air flow. Firstly, thanks to the root mean square error (RMSE = 4.5 °C), indicating good agreement between the numerical and experimental temperatures of the heat transfer air passing through the receiver, the thermal performance of this dryer seems evident. Then, experimental tests carried out on the dryer, both empty and loaded, using Clemson Spineless okra, made it possible to determine a hot air temperature level (40 °C - 60 °C) recommended for drying okra without denaturing its trace elements. Thus, the influence of the shapes (cylindrical and longitudinal) and sizes (1 cm, 1.5 cm, and 2 cm) of the dried okra pieces was noted. Also, the diffusion coefficient values $(16.49 - 22.72) \times 10^{-9} \text{ m}^2 \text{ s}^{-1}$ and $(6.24 - 15.59) \times 10^{-9} \text{ m}^2 \text{ s}^{-1}$ for the cylindrical and longitudinal slices, respectively, and the drying rate quantifying the water lost in these slices yielded promising results. Finally, observations were made on the appearance of the dried okra pieces, including their color retention, properties, and dryness. Tasting a delicious and appetizing sauce made with okra dried using the new dryer also indicated satisfaction with the performance of the CPC dryer.

Key words: CPC solar dryer, optimal temperatures, Clemson Spineless, diffusion coefficient, drying speed, appearance of dried slices.

1. Introduction

In third world countries where there is constant sunshine, solar drying is the most commonly used technique for preserving agricultural products. Unfortunately, it is a technique for processing and preserving products of mediocre quality.

Studies have been conducted to correct the weaknesses of open-air solar drying in particular and those of flat-plate solar dryers [1-3]. The results of these improvements, including the desired temperature level and drying time, remain unsatisfactory [4].

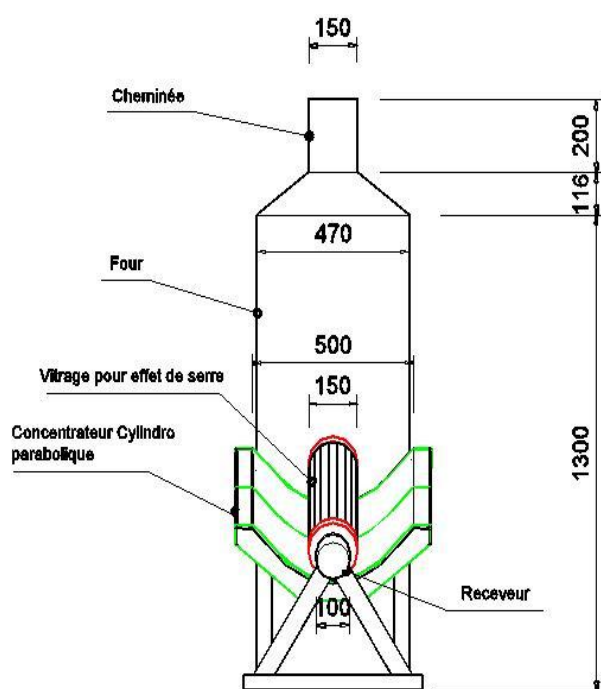
Thus, replacing the flat plate collector with a CPC type collector is a viable technical and economic

compromise for improving the performance of indirect solar dryers [5] and a solution for improving the thermal performance of an indirect solar dryer and reducing the long drying time [4]. To confirm the performance offered by such a thermal converter attached to an oven, tests were carried out on the drying of a variety of Clemson Spineless okra. The results are presented here and compared with data from the literature.

2. Materials and Operating Procedures

2.1 Materials

Fig. 1 shows the schematic diagram and experimental setup of the CPC-type cylindrical parabolic solar dryer.



Synoptic diagram of the new solar dryer

Fig. 1 Images of the indirect solar dryer with CPC collector.

2.2 Operation

Fig. 1 shows a new solar dryer consisting of a parabolic concentrator with a surface covered with aluminium foil, an aperture of 50 cm, a length of 100 cm, a focal length of 10 cm, and a depth of 15.6 cm.

Indeed, the optimal dimensions of the concentrator indicated above would produce maximum useful energy and reduce optical and thermal losses, which are common in such devices.

However, a large absorber results in enormous thermal losses [6] and, of course, high manufacturing costs!

The receiver is made of thin rolled steel, 10 cm in diameter and approximately 140 cm long, placed in the focal zone of the concentrator. It consists of two coaxial cylindrical tubes, the first of which is made of glass, providing the greenhouse effect, and the second, which acts as an absorber of reflected solar flux, is made of blackened steel [6].

Consequently, the presence of a vacuum in the annular space between the absorber and the glass reduces convection losses [7]. The entire unit is tilted at an angle of 12° to the horizontal to promote natural



Dryer at the end of use

convection of the drying air towards the oven outlet.

This tubular configuration of the receiver makes it easier for the sensor to track the sun, which is not always automatic, so that the incident solar beam, which is inclined relative to the axis of symmetry of the receiver, is focused correctly!

The oven with insulated walls is a rack with racks. A door at the back of the drying chamber facilitates access to the racks.

2.3 Procedure

There are several notable varieties and species of okra, including Clemson Spineless (Fig. 2), which was used for the solar dryer experiments described in this article. This early variety is commercially available and produces optimal yields during the off-season, when it performs very well due to the high prices of okra at that time. It is also highly productive (20 to 30 t/ha).

It was purchased around 6 a.m. in a field. Upon arrival at the experiment site, the samples were sorted, and the stems and cap tips were cut off. We then proceeded to make various cuts, including longitudinal

and cylindrical slices (lengths or heights: 1 cm, 1.5 cm, and 2 cm). Finally, these slices were weighed, lined up

on racks, and placed in the oven. All of these steps are illustrated in Fig. 2.



Fig. 2 Drying stages.

3. Analysis of Results

3.1 Dry Mass and Initial Water Content

To obtain the dry mass, the okra slices are dried in an oven set at 70 °C for 24 hours to remove moisture, after which their mass (m_s) is measured [8]. Thus, the initial water content on a dry basis X_0 is obtained using the following Equation (1).

$$X_0 = \frac{m_0 - m_s}{m_s} \quad (1)$$

3.2 Water Content and Absolute Moisture Content of Okra

The proportion of water by weight of dry matter $X(t)$, at a given moment in the dehydration process, is defined by the corresponding mathematical Equations (2) and (3). The water content on a wet basis (X_h) is defined by the equation of Monneveux (4) [9].

$$X(t) = \frac{m(t) - m_s}{m_s} \quad (2)$$

<=>

$$X(t) = \frac{m(t)(X_0 + 1) - m_0}{m_0} \quad (3)$$

In these expressions, $m(t)$ is the mass of okra at each drying time t and m_s is its dry mass or anhydrous mass.

$$X_h = \frac{m(t) - m_s}{m_0} \times 100 \quad (4)$$

where m_0 is the initial (or fresh) mass of the okra.

These water contents are defined by the following Equations (5) and (6):

$$X = \frac{X_h}{1 - X_h} \quad (5)$$

and

$$X_h = \frac{X}{1 + X} \quad (6)$$

3.3 Drying Speed (Evaporation Rate)

The value of the evaporation rate is determined by Equations (7), (8), and (9), which are used to quantify

this process.

$$\text{At } t = t_0, V_0 = \frac{X_1 - X_0}{t_1 - t_0} \quad (7)$$

$$\text{At } t = t_i (i = 1, 2 \dots n-1) V_i = \frac{X_{i+1} - X_{i-1}}{t_{i+1} - t_{i-1}} \quad (8)$$

$$\text{At } t = t_n, V_n = \frac{X_n - X_{n-1}}{t_n - t_{n-1}} \quad (9)$$

3.4 Diffusion Coefficient

The diffusion coefficient is a measure that indicates the speed and ease with which water migrates through a material. It quantifies the amount of water that passes through a given surface of a product during drying [7].

It is obtained using the solution by analytically solving Fick's second law for biological products, taking into account the cutting geometry of these products [10].

Cylindrical section

$$\frac{\partial X}{\partial t} = \frac{1}{r} \left(\frac{\partial}{\partial r} \left(D r \frac{\partial X}{\partial r} \right) \right) \quad (10)$$

Longitudinal section

$$\frac{\partial X}{\partial t} = D \frac{\partial^2 X}{\partial x^2} \quad (11)$$

Equations (10) and (11) are solved using equalities (12) and (13).

Cylindrical cutting

$$MR = \frac{X_t - X_{eq}}{X_0 - X_{eq}} = \frac{4}{\beta^2} \exp \left(-\frac{\beta^2 D t}{r_c^2} \right) \quad (12)$$

Longitudinal cutting

$$MR = \frac{X_t - X_{eq}}{X_0 - X_{eq}} = \frac{8}{\pi^2} \exp \left(-\frac{\pi^2 D t}{4 L^2} \right) \quad (13)$$

In these relationships, we have:

X_i (average water content), X_{eq} (equilibrium water content), and X_0 (initial water content), all expressed in g/g_{wat}erms.

D (m².s⁻¹) is the diffusion constant, r_c (m) is the radius of the cylindrical sample, L (m) is the length of the cut, and t (s) is the drying time.

3.5 Validation Criteria

Several statistical parameters can be used to validate the results of an experiment. In this article, the RMSE

(root mean square error) established by Equation (14) allows us to confirm our results.

$$RMSE = \sqrt{\frac{1}{N} \sum_{i=1}^{i=N} (T_{1,i} - T_{1,sim})^2} \quad (14)$$

where $T_{1,i}$ and $T_{1,sim}$ are the experimental and theoretical values of the air temperatures at the furnace inlet, respectively.

4. Results and Discussion

4.1 Heat Transfer Fluid Temperature Levels

4.1.1 At the CPC Crossing

Fig. 3 shows the simulated temperature evolution of the heat transfer fluid, in natural convection inside the absorber tube, as a function of the length of the tube. This evolution was observed by Chekirou et al. [11] on a 12 m long cylindrical-parabolic collector.

The simulated temperature of the heat transfer fluid circulating inside the absorber tube changes linearly depending on the length of the tube and the local time of the sun. We recorded an average temperature of 50 °C between 8 a.m. and 4 p.m.

4.1.2 Inside the Dryer

The average temperatures recorded on the racks,

numbered from bottom to top of the box, were 61.19 °C, 58.65 °C, and 57.09 °C, respectively, with maximum temperatures of 75.2 °C, 65.1 °C, and 63.2 °C for each rack.

The data in the literature agree on a temperature range of 43.5 °C to 60 °C for high-quality drying, ensuring better preservation of okra nutrients [12]. Our results are in perfect agreement with the literature, which also recommends this temperature range for okra drying.

In addition, the drying air exchanges heat with the inner wall of the oven as it rises. This regularly cools the temperature of the drying air.

The curves in Fig. 4 show the air temperature profile inside the dryer chamber.

There is a decrease in the temperature of the drying fluid at the racks, from rack n^o.1 to the last one, located at the top, in the direction of air flow, due to energy exchanges between the air and the oven wall.

4.1.3 Validation of Results Obtained

To validate the results obtained, we calculated the RMSE (root mean square error) between the simulated air temperatures at the furnace inlet and those obtained experimentally.

It is 4.5 °C. Fig. 5 shows the agreement between these values.

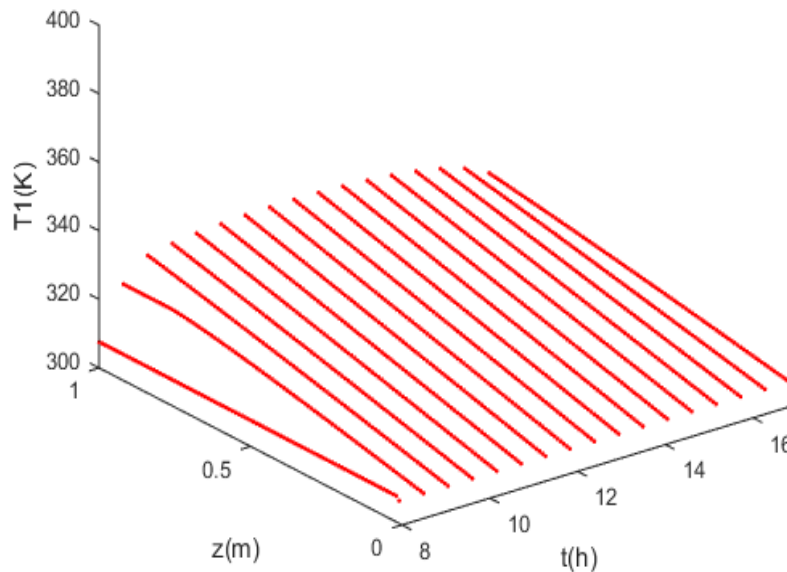


Fig. 3 Simulated fluid temperature in simple convection inside the tubular receiver of the CTP-type heat converter.

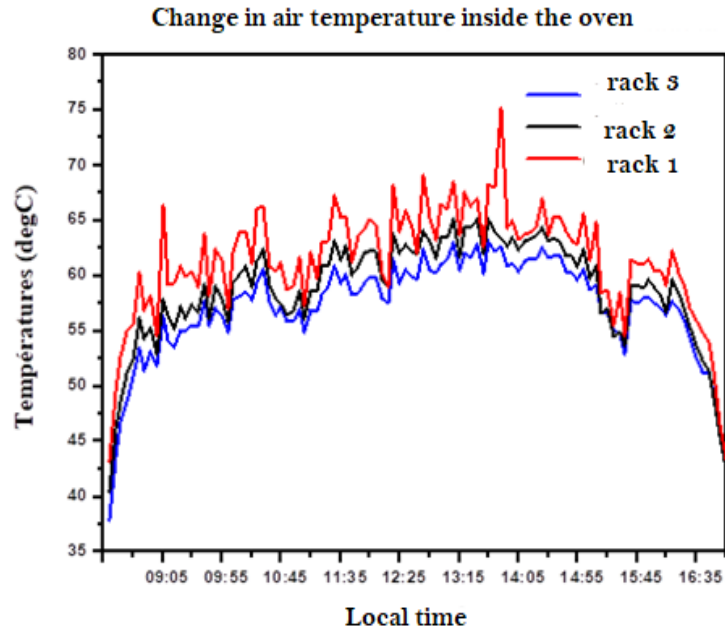


Fig. 4 Air temperature profile at the crossings of the racks inside the oven.

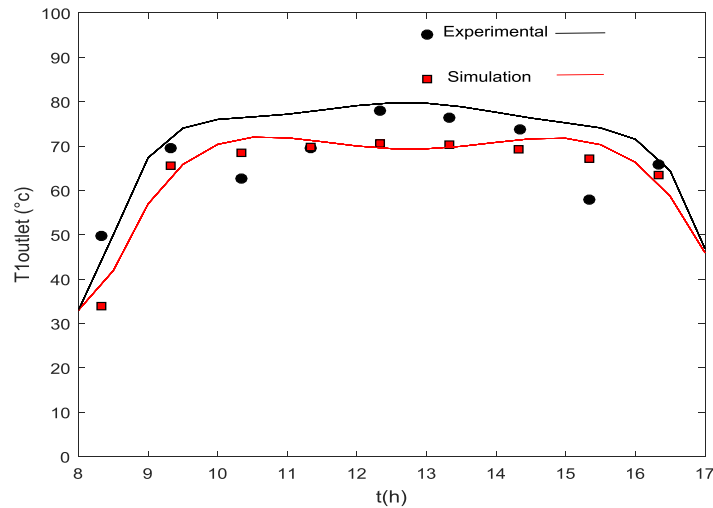


Fig. 5 Evolution of simulated and measured fluid temperatures at the inlet to the drying cage.

4.2 Dry Mass and Initial Water Content of Okra

A quantity of (107.52 ± 0.01) g of fresh okra mass was left for 24 h in an oven at a temperature of 70°C . Once the period was over, the dry mass of the sample was recorded as: (12.82 ± 0.01) g, representing 94.7 g of water removed. With the initial mass recorded, the water content was obtained using Equation (1). It was $7.38 \text{ g}_{\text{water}}/\text{g dry weight}$, or 88.07% wet weight. This value is consistent with data in the literature,

according to which the initial moisture content of okra is between 88 and 90%, and the final moisture content ranges from 5 to 10% (wet basis) [13].

4.2.1 Influence of Cutting Shapes

Two different types of slices (round and longitudinal), of different sizes (height and length of 1 cm and 2 cm), were prepared. The initial mass of the product before drying was 207.7 g per slice, for a total of four slices.

Table 1 Results from the first day of okra drying.

Cutting shapes	Initial mass (in g)	Evacuated water mass (g)	Final mass (g)
Round, 1 cm	207.7	127.5	80.2
Round, 2 cm	207.7	107.6	100.1
Length, 1 cm	207.7	170.4	37.3
Length, 2 cm	207.7	158.0	49.7

Table 2 Results of okra drying on the second day.

Form of cuts	Initial mass (in g)	Evacuated water mass (in g)	Final mass (in g)
Round, 1cm	78.8	56.3	22.5
Round, 2cm	98.1	74.9	23.2
Length, 1cm	36.3	14.0	22.3
Length, 2cm	48.2	25.8	22.4

Drying began at 8:30 a.m. and ended at 5:30 p.m. on the first day, and then continued the following day from 8:05 a.m. to 5:05 p.m., during which time the sun was not obscured by cloud cover. The mass results of the samples from this operation are presented in Table 1.

According to the results in Table 1, the longitudinal cuts of okra quickly released more water than the cylindrical slices; thus, they dried faster than the latter.

Furthermore, the amount of water released depends on the shape of the cut and its size (length and/or height). This is confirmed by the results shown in Table 2.

According to the results in the previous tables, the dried okra pieces had different final weights due to their shapes and sizes.

The amounts of water extracted from these pieces on the first day were greater than on the following day. A similar observation was made by Wankhade et al. [14].

There was a much greater decrease in evaporation on the second day than on the previous day.

The phenomenon reversed on the second day of drying, in terms of the rate of water evaporation from the dried okra pieces. The slices that had dried out the most on the first day dehydrated less the next day. This is inevitably the result of physical deformations, in particular the shrinkage of the structure of the samples and at the level of the pores, which were blocked by soluble nutrients (sugar and salt). An imaginary drying

line, or “drying front”, formed between the point where the hot air entered and the product’s exit surface, beyond which the air was saturated [15].

4.2.2 Influence of Cut Shape on Drying Speed

Fig. 6 shows the impact of the cut shape on the drying speed. These correspond to longitudinal and cylindrical cuts (length or height: 1 cm and 1.5 cm). Drying speeds are shown as a function of elapsed time.

These graphs (a and b) show that the longitudinal cut dried faster at the beginning of the drying process than the cylindrical cut. This is due to the larger surface area for simultaneous heat and water exchange between the air and the product in the longitudinal slice.

After approximately 4 hours of drying, the situation is reversed until the end.

In order to obtain more accurate results, a third experiment was conducted. Two cuts were made, one cylindrical (1 cm and 1.5 cm, high) and the other longitudinal, dividing the sample into two sections 1 cm and 1.5 cm long.

Two samples, one cylindrical (1 cm) and one longitudinal (1 cm), were dried in the open air. The initial mass of each sample was $66.0 \text{ g} \pm 0.1 \text{ g}$.

The experiment began on the first day at 9:00 a.m. and continued until 5:00 p.m., resuming the following day at the same time. The masses were weighed every 30 minutes. Table 3 below summarizes the masses (final and dry) and final water content of the samples.

Table 3 Summary of the drying process carried out.

Type of drying	Sections	Final weights (g)	Dry masses	X_f (g _{eau} /g _{ms})
Samples from the dryer	Length, 1 cm	7.2 ± 0.1	6.8 g ± 0.01 g	0.05
	Length, 1.5 cm	7.8 ± 0.1	6.67 g ± 0.01 g	0.16
	Round, 1 cm	8.2 ± 0.1	7.29 g ± 0.01 g	0.12
	Round, 1.5 cm	11.2 ± 0.1	6.94 g ± 0.01 g	0.61
Natural drying	Length, 1 cm	8.2 ± 0.1	7.65 g ± 0.01 g	0.07
	Round, 1 cm	8.7 ± 0.1	7.57 g ± 0.01 g	0.14

The results in Table 3 show that cutting the okra lengthwise, dividing it into two parts, dries faster than cutting it into 1 cm thick cylindrical slices. We can therefore conclude that okra dries faster when cut in a way that opens up the skin as much as possible. Opening the skin seems to prevent water vapor from accumulating in the product, thereby slowing down water transfer and air renewal inside the okra. The opening also increases the air-product exchange surface area. The product exchange surface area plays a key role in assessing the amount of heat exchanged. The larger the exchange surface area, the greater the possibility that the product will receive more heat [16]. This phenomenon is much more pronounced when the sample size is increased, as can be seen in Fig. 6.

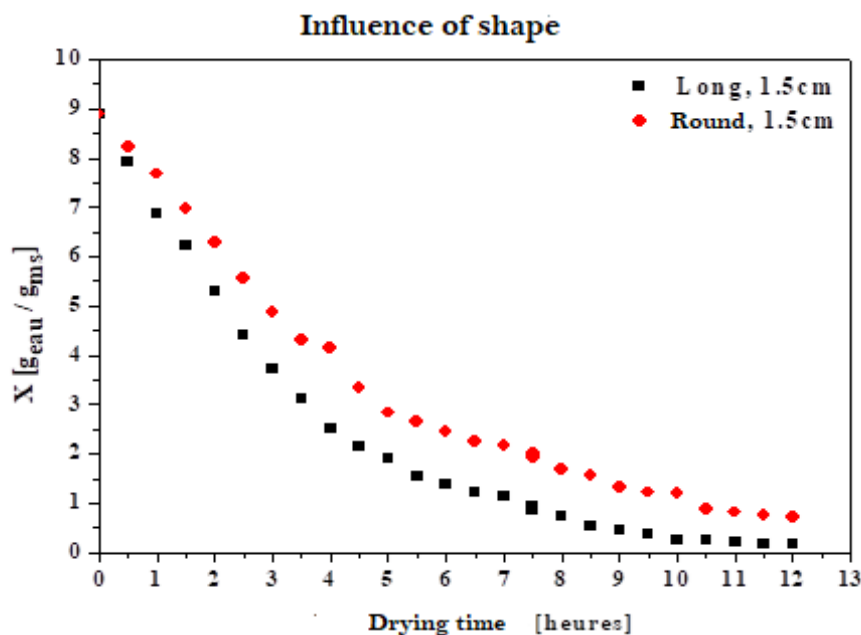
4.2.3 Influence of Drying Methods on the Kinetics of Okra Drying

The results in Table 3 and Figs. 7 (a and b) show the

influence of drying methods, between natural drying and drying in a dryer. Two types of cuts were made: longitudinal cuts (1 cm) and cylindrical cuts (1 cm and 1.5 cm). We observe that samples of short length or height (1 cm), for both cuts (longitudinal and circular), dry faster in the open air than in the dryer.

However, the phenomenon is reversed when the size of the slices is increased. Thus, okra cut into cylindrical slices 1.5 cm thick dries faster in the dryer than in the open air, as shown in Fig. 7c below.

Looking at this graph, we note that after approximately 8 hours of exposure, the amount of water removed from the 117.1 g of okra initially introduced is 99.7 g and 77.4 g in the dryer and natural drying, respectively. This confirms the effectiveness of drying using the dryer compared to natural drying in terms of the amount of water lost and the duration of the operation.

**Fig. 6** Significant influence of the cutting shape on drying kinetics.

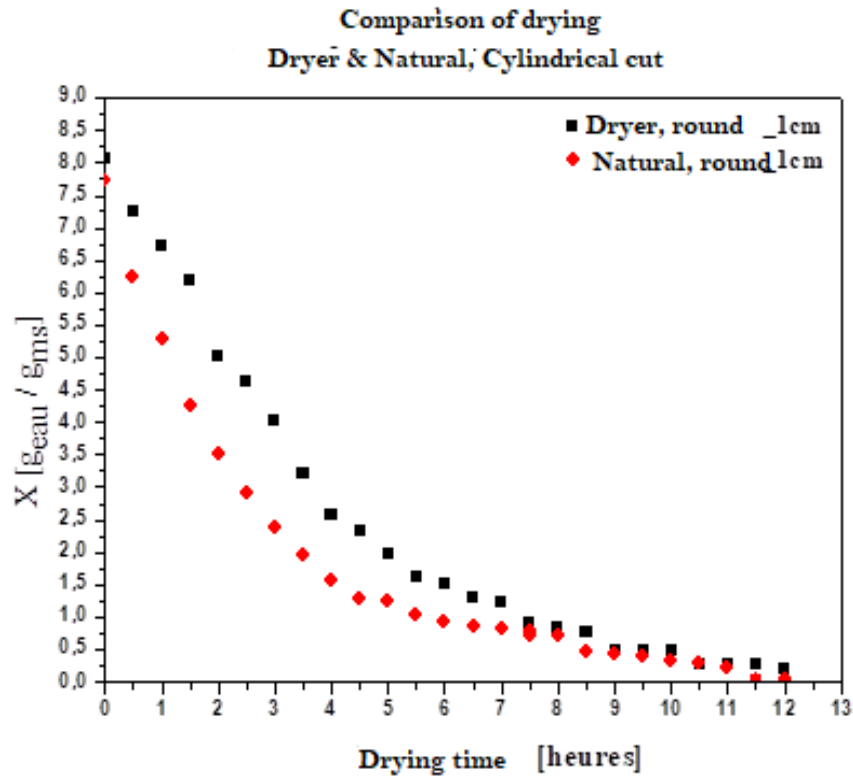


Fig. 7a Influence of drying method (natural or dryer) on water content.

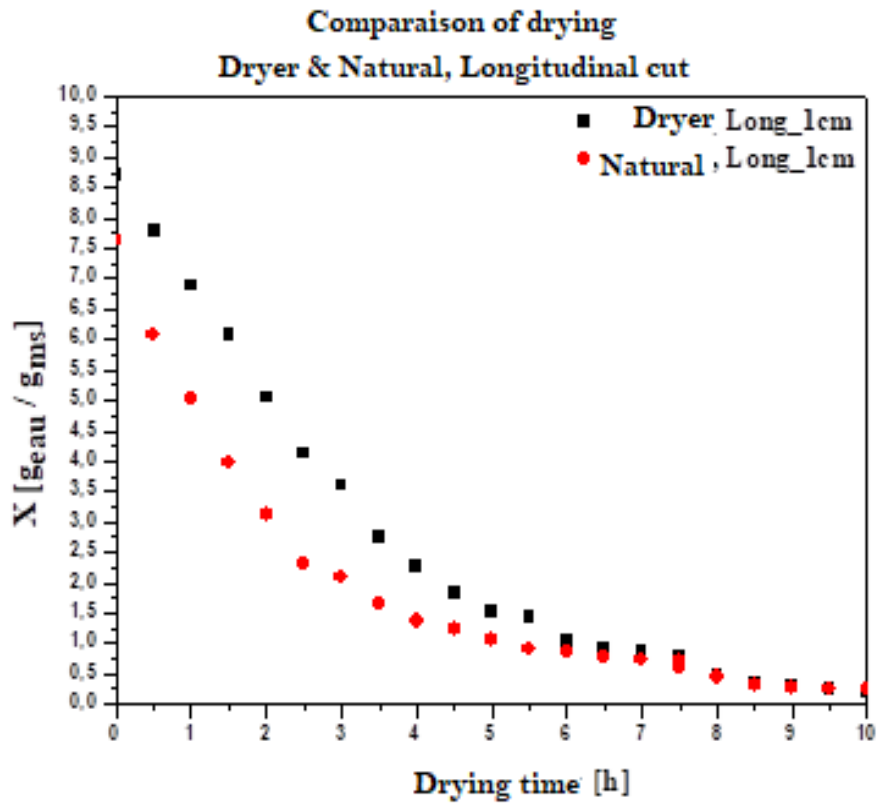


Fig. 7b Drying methods (natural and dryer). Longitudinal cutting.

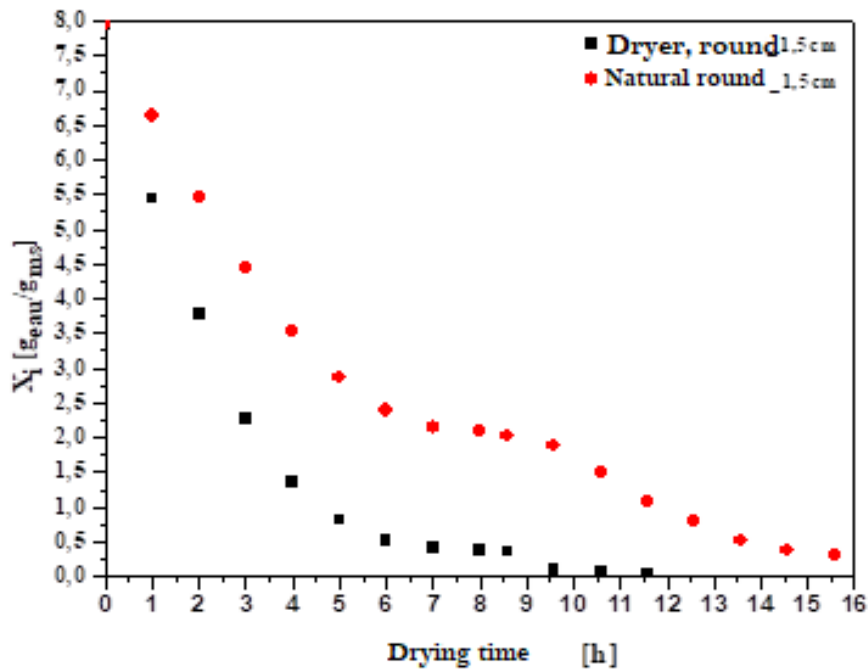


Fig. 7c Influence of drying method on water content over time.

Influence of the position of the racks on the drying speed

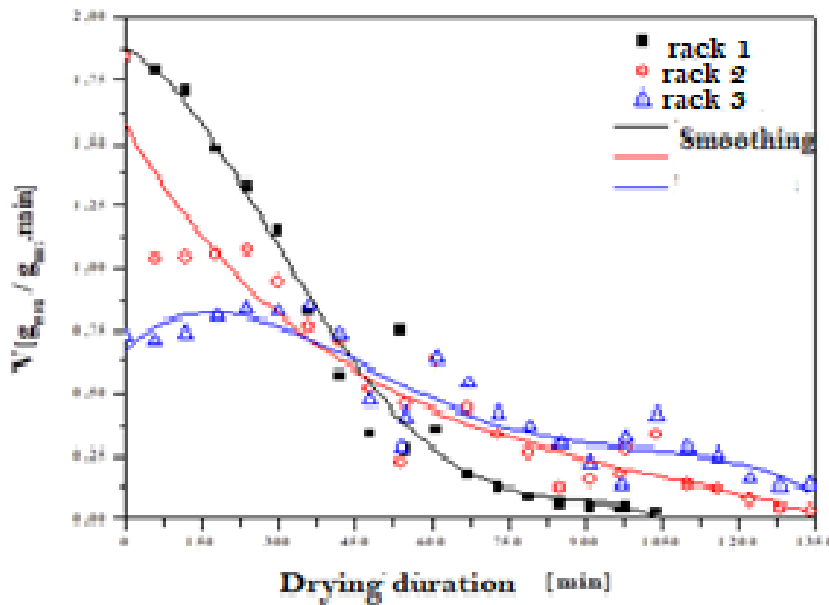


Fig. 8 Influence of rack position on drying.

This could be justified by the difference in temperature between the hot air in the dryer and the ambient air used for natural drying. This is because the temperature of the drying air is the key parameter for drying okra slices [14]. This finding was confirmed by Garnier [17]. Increasing the air temperature reduces drying time by 75% [18].

4.2.4 Influence of Product Location on Drying Speed

The position occupied by a product to be dried in an oven has a significant effect on the drying process, particularly the drying speed, as shown in Fig. 8.

The three smoothing curves all show two phases and two periods:

During the first exposure phase (0 to 450 minutes), the drying rate decreases. Furthermore, during this period, the drying rate of the okra slices is higher on rack 1 than on rack 2, and the same is true for rack 2 compared to rack 3. The results recorded in Table 4, regarding the final masses of the samples at the end of the first day of drying, confirm this observation. The curves showing the evolution of the water content (Fig. 9) confirm this.

During the second period (beyond 450 minutes), The drying rate during the drying process of okra pieces spread out on racks reverses as the samples shrink, which hinders the migration of water to the outside.

Looking at these curves, rack n°1, the first to receive the drying air just as it enters the oven, evacuates its moist contents fairly quickly, as does rack n°2, which in turn reproduces the same phenomenon, and so on

until the last rack at the top of the oven. This situation shows that the temperature of the hot air decreases as it passes through the loaded racks. In fact, the air is conveyed through the cabinet from bottom to top. As air moves from a lower rack to an upper rack, its temperature decreases and its humidity level increases. This causes an increase in water vapor pressure in the air and a decrease in exchange potential, defined as the difference between the vapor pressure at the surface of the product and the water vapor pressure in the air [19].

Three racks were loaded, each with $304.0 \text{ g} \pm 0.1 \text{ g}$ of okra, cut into rounds and placed in the oven. The change in water content as a function of drying time is shown in Fig. 9.

This experiment provided an opportunity to monitor the weight loss of the samples placed on the racks. The results obtained are summarized in Table 4:

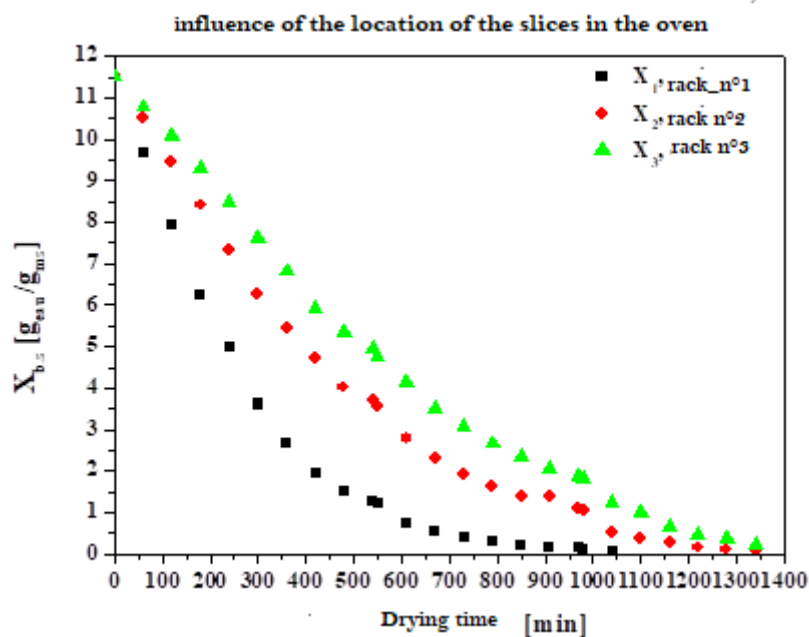


Fig. 9 Influence of the location of a drying rack on the water content of the product.

Table 4 Results of the drying process.

Rails	Final weights, 1st day	Anhydrous masses	Drainage water
Rail 1	55.4 g	25.5 g	278.5 g
Rail 2	114.1 g	26.6 g	277.4 g
Rail 3	145.2 g	29.8 g	274.2 g

Table 5 Diffusion coefficient values of okra slices.

Cutouts	Dimensions (cm)	D ($\times 10^{-10} \text{ m}^2 \cdot \text{s}^{-1}$)
Cylindrical	h = 1	22.72
	h = 1.5	20.48
	h = 2	16.49
Longitudinal	Length = 1	6.24
	Length = 2	15.59

Table 6 Diffusion coefficient of okra in the present work and in the literature.

Authors	D ($\times 10^{-10} \text{ m}^2 \cdot \text{s}^{-1}$)	Cutouts	Dimensions
Present work	16.49 - 22.72	Cylindrical	R = 0.7 cm
G. Ouedraogo	6.16	Longitudinal	
I. Doymaz	4.27 - 13.0	Whole okra	
Dadali et al.	20.52 - 86.17		

4.3 Diffusion Coefficient Values

The data collected following the experimental tests recorded in Table 5 led to the determination of the diffusion coefficients of the longitudinal and cylindrical sections of okra.

The diffusion coefficient values obtained allow the chosen drying technique to be evaluated. The higher the diffusion coefficient, the faster the transfer and the quicker the products dry. In this study, the diffusion coefficient of the cylindrical cut demonstrates this.

Diffusion was faster in the low-height samples. This shows that diffusion occurs in the direction of the drying air flow.

In longitudinal samples, the phenomenon is reversed. The amount of water contained in a 1 cm longitudinal cut is less than that in a 1.5 cm cut because the length of the slice is shorter.

Diffusion is greater in okra pieces with a circular cross-section than in those with an elongated shape. This is because the arrangement of the slices in longitudinal slits on the racks in the oven slows down the spread of heat through the skin during drying [20].

Furthermore, longitudinal samples have less water to remove than cylindrical pieces; this partly explains the D values (diffusion coefficient).

A comparison of the results obtained with those in the literature presented in Table 4 allows them to be evaluated.

Multiple reasons could be cited to explain the

differences in diffusion coefficient values, including:

- Drying conditions are not the same; some drying is done using microwaves and others using sunlight,
- The effects of temperature on the structure of a product to be dried [20-21],
- The thickness of the sample plays an important role in drying [22-23],
- Okra varieties may exhibit different phenomena during drying, as may the types of drying equipment used,
- Overall operating conditions and other uncontrolled parameters.

4.4 Characteristics of the Dried Product

The okra samples from the dryer were used to make a sauce, which some members of our laboratory tasted. The samples were found to be clean, dry, and delicious. The images in Fig. 10 illustrate this.

5. Conclusion

A cylindrical solar collector was integrated into an oven, forming an indirect solar convection dryer. An experimental campaign was conducted using this dryer to dry okra of the Clemson Spineless variety. The following promising results were obtained:

- A correlation between the simulated and experimental temperatures of the heat transfer fluid at the oven inlet. This was achieved by calculating the RMSE (root mean square error).



Fig. 10 Tasting the sauce made with okra dried using the new dryer.

- The temperature level of the air circulating inside the oven is recommended for drying okra without denaturing its nutrients.
- The dried okra pieces yielded interesting diffusion coefficient values when taken into account, indicating the performance of the current solar dryer.
- The appearance of the dried okra pieces also indicated the performance of the new solar dryer compared to pieces dried in the open air.

We still need to test this solar dryer on various vegetables that are frequently consumed in the Central African Republic.

References

- [1] Dissa, A. O., Desmorieux, H., Bathi ðo, D. J., and Koulidiati, J. 2011. "Analytical Estimation and Modeling of Water Diffusivity during Convective Drying of Mango Considering Two Diffusion Zones." *J. Soc. Ouest-Afr. Chim.* 31: 21-34.
- [2] Abene, A., Dubois, V., and Le Ray, M. 2004. "Study of a Solar Air Flat Plate Collector, Use of Obstacles and Application for the Drying of Grape." *Journal of Food Engineering* 65 (1): 15-22. doi:10.1016/j.2004.
- [3] Malenguinza, S. 2012. "Optimization of the Double Glazed Collector by the Design of Experiments Method." Ph.D. thesis, University of Abomey Calavi, Benin.
- [4] Pakouzou, B. M., Ky, M. S. T., Gbembongo, S. T., Ou ðraogo, G. P., Mackpayen, O. A., Dianda, B., Kam, S., and Bathi ðo, D. J. 2017. "Thermal Performance of a Receiver Located in the Caustic Area of a Cylindro-Parabolic Solar Concentrator." *Physical Science International Journal* 16 (3): 1-14. PSIJ.37156; ISSN:2348-0130. doi:10.9734.
- [5] Pakouzou, B. M., Bathi ðo Dieudonn é J., and Bassia, J.-M. 2013. "Design of a Cylindro-Parabolic Collector Applied to an Agricultural Solar Dryer." *Journ ées Internationales des Thermiques (JITH), Marrakech, Morocco.*
- [6] Magloire Pakouzou, B., Germain Ou ðraogo, P. W., Bokoyo, V. B., Ousman, M., Auguste Mackpayen, O., Kabor é B., and Kam, S. 2022. "Experimentation of the Solar Dryer with Parabolic Trough: Drying of Okra." *International Journal of Advanced Engineering Research and Science (IJAERS)* 9 (1): 34-41. Available: <https://ijaers.com/doi:https://dx.doi.org/10.22161/ijaers.91.2>
- [7] Guerraiche, D., Benderradji, A., and Benmoussa, H. 2011. "Optical and Geometrical Factors Characterizing a Parabolic Trough Concentrator." *Revue des Énergies Renouvelables* 14 (2): 229-38.
- [8] AOAC. 1990. (Association of Official Chemists). *Official Methods of Analysis*. Washington AC, 934-06.
- [9] Monneveux, P. 1991. "Quelles strat égies pour l'am élioration g énéique de la tol érance au d éficit hydrique des c éréales?" In *Plant Breeding for Adaptation to Arid Environments*, edited by Aupelf-Uref. Montrouge: John Libbey Eurotext, pp. 165-86.
- [10] Wang, N., and Brennan, J. G. 1992. "Effect of Water Binding on the Drying Behavior of Potato." *Drying* 92: 1350-9.
- [11] Chekirou, W., Boukheit, N., and Kerbache, T. 2007. "Diff érents modes de transfert de chaleur dans un absorbeur d'un

- concentrateur solaire cylindro-parabolique.” In *Revue des Énergies Renouvelables ICRES-07*, pp. 21-28. Tlemcen.
- [12] Pendre, N. K., Nema, P. K., Sharma, H. P., Rathore, S. S., and Kush-wah, S. S. 2011. “Effet of Drying Temperature and Slice Size on Quality of Dried Okra (*Abelmoschus esculentus* L. Moench).” *Journal of Food Science and Technology* 49 (3): 378-81.
- [13] Shivhare, U. S., Gupta, A., Bawa, A. S., and Gupta, P. 2010. “Drying Characteristics and Product Quality of Okra.” *Drying Technology* 18 (1 & 2): 409-19. doi:10.1080/07373930008917712.
- [14] Wankhade, P. K., Dr. Sapkal, R. S., and Dr. Sapkal, V. S. 2013. “Drying Characteristics of Okra Slices on Drying in Hot Air Dryer.” *Procedia Engineering* 51: 371-4. doi:10.1016/j.proeng.01.051.
- [15] Garango, L. T. 1985. “Conception, Realization and Study of a Solar Dryer: The ‘TUNNEL.’” Centre d’Études et de Recherches sur les Énergies Renouvelables (CERER), University of Dakar.
- [16] Ouoba, K. H., Zougmor é F., Sam, R., Toguyeni, A., and Desmorieux, H. 2014. “Characterization of Okra Convection Drying, Influence of Maturity.” *Food and Nutrition Sciences* 5: 590-7. doi.org/10.4236/fns.56069.
- [17] Garnier, C. 2014. “Mod éisation Num érique des écoulements Ouverts de Convection Naturelle au sein d’un Canal Vertical Asym étriquement Chauff é” Université Pierre et Marie Curie, LIMSI.
- [18] Mourad, M. 1992. “Contribution à l’étude des cinétiques de déshydratation et d’évolution de la qualité commerciale de ma ï au cours du séchage en lit fluidisé à flotation.” Th èse de doctorat, Ecole Nationale Supérieure d’Ingénieurs de Génie chimique de Toulouse. INP.
- [19] Kiranoudis, C. T., Maroulis, Z. B., and Marinos, D. 1992. “Mol Selection Air Drying of Foods.” *Drying Technology* 92: 785-93.
- [20] Doymaz, I. 2005. “Drying Characteristics and Kinetics of Okra.” *Journal of Food Engineering* 69: 275-9.
- [21] Nadir, N. 2007. “Research of the Optimal Conditions of Operation of a Solar Dryer.” Magister thesis, Kasdi Merbah University, Ouargla.
- [22] Magloire Pakouzou, B., Landry M’Bouana, N., Thierry Ky, M. S., M’Boliguipa, J., and Joseph Bathi éo, D. 2021. “Experimental Evaluation of Thermals Performances of The Solar Dryer with Parabolic Trough Collector Current” *Journal of Applied Science and Technology* 40 (19): 1-9. Article No. CJAST.71833. ISSN:2457-1024. doi:10.9734.
- [23] Ouedraogo, G. W. P., Kabor é B., Pakouzou, B. M., Sawadogo, K., Zoma, V., Kam, S., and Bathi éo, D. J. 2021. “Thermal Analysis of a Solar Dryer with Parabolic Collector.” *Science Research* 9 (6): 127-31. doi:10.11648/j.sr.20210906.15. ISSN:2329-0935 (Print); ISSN: 2329-0927.